

Chapter 14

Imaging Neural Architecture in Brainbow Samples

Douglas H. Roossien and Dawen Cai

Abstract

The fluorescent protein revolution has made the light microscope the most widely used tool for studying biological structure from the single-molecule to whole organism scales. However, traditional approaches are limited in their ability to resolve components in highly complex structures, such as the brain. In recent years, this limitation has been circumvented by the development of multicolor labeling methods, termed Brainbow. Brainbow tools rely on site-specific recombinases to make stochastic “choices” between different combinations of fluorescent proteins so that structures in close proximity to one another can be resolved based on their color profile. These new approaches, however, call for more refined methods of sample preparation and imaging optimized for multispectral imaging, which are presented here. The most robust approach for generating useful Brainbow data combines immunohistology with multispectral laser scanning confocal microscopy. This chapter, therefore, focuses on this particular technique, though the imaging principle discussed here is applicable to other Brainbow approaches as well.

Key words Brainbow, Multispectral imaging, Immunohistology, Neuroscience, Development, Confocal microscopy, Linear unmixing

1 Introduction

The impetus for the original Brainbow designs was the desire to comprehensively study neuronal circuitry in the brain using the light microscope. Individual neurons in the brain can have immensely complicated morphologies, which can confound visualizing how processes from different neurons integrate into functional circuits. Traditional light microscopy approaches for tracing whole neuronal morphologies used labeling methods such as the Golgi stain, single-cell dye injections, or genetic expression of fluorescent proteins, but all rely on sparse labeling of cells to be able to unambiguously identify the fine, often interwoven, processes as belonging to a particular neuron. The first Brainbow designs adopted by Livet and colleagues therefore sought to label neurons in close proximity with unique color labels by expressing a different random combination of fluorescent proteins (FPs) in each neuron [1]. To achieve this they utilized the Cre/Lox site-specific

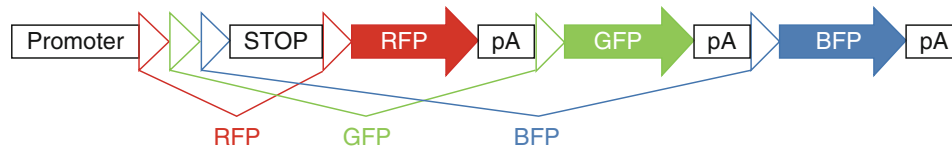


Fig. 1 Schematic of a generic Brainbow construct. Expression of Brainbow is prohibited by a transcriptional stop signal just downstream to the promoter. Alternatively, a default epitope or FP followed by a polyadenylation (pA) signal can be used. This is flanked on the 5' side by each of three incompatible recombination target sites (e.g., Lox or Frt sites) shown here as *red*, *green*, and *blue triangles*. Just 3' to the stop signal is the first of the three incompatible target sites. If recombination occurs between these two sites, the stop signal is removed and the first FP is expressed (RFP in this example). The pA prohibits transcription of the other FPs remaining in the cassette. The second target site (*green triangle* here) is placed just after the first pA. If recombination occurs between these target sites, the stop and the RFP are excised resulting in GFP expression. The same design is repeated for BFP expression

recombination system, notably the inability of Cre to excise/invert DNA sequences flanked by mutated (or “incompatible”) Lox sites [2]. By placing three incompatible Lox sites 5' to a default FP and flanking each of the three subsequent FPs with one of the three Lox sites, stochastic recombination occurs between one pair of the incompatible Lox sites and excludes further recombination (*see* Fig. 1). The default FP is removed, and the resulting product expresses only one of the remaining FPs due to polyadenylation signals after each FP coding sequence (*see* Fig. 1). Color outcome diversity was then increased by integrating multiple copies of the Brainbow construct into the mouse genome, effectively mimicking a television screen mixing red, blue, and green hues in each neuron [3]. Since the original Brainbow, several different modifications have been made to either improve the system or to adapt it to particular needs/biological systems. Some examples include choosing brighter FPs with more easily separated emission spectra [4], cellular compartmentalization of FPs [5], different recombinases [4, 6, 7], and different species/vectors [4–6, 8–12]. See Weissman and Pan [13] for thorough review of available Brainbow tools. Regardless of the modification, almost all depend on stochastic recombination events occurring independently in each cell.

For the second generation of Brainbow tools [4], membrane-bound instead of cytoplasmic FPs were used to produce homogeneous labeling even in the finest axonal and dendritic structures. FPs were specifically chosen to allow for combinatorial immunohistology. For this approach, each FP serves as an antigen for a different non-cross-reactive primary antibody. Immunolabeling these samples produces much higher fluorescence intensity for two reasons: (1) the fluorophores conjugated to secondary antibodies are typically brighter than FPs and (2) the use of polyclonal primary antibodies “amplifies” the signal by attaching multiple fluorophores to each FP. This is especially important for plasma membrane-bound FPs, which can appear dim due to the reduced volume of FP within and near an

illumination plane. There are several other distinct advantages to the antibody amplification approach: the fluorophores can be specifically chosen for compatibility with the optics of available microscopes; multispectral imaging is easier with dyes than FPs as they span wider emission spectral range, provide high signal-to-noise ratio, and are more resistant to photobleaching. While the choice of which Brainbow tool is best suited for the biological question at hand is beyond the scope of this chapter, Table 1 provides a comprehensive list of currently published Brainbow tools and which of them are compatible with antibody amplification. Noncompatibility is due to common antigenicity of FPs in the system; for example, EGFP and EYFP both serve as antigen for the same primary antibody. If the specific Brainbow tool of choice is not antibody compatible, the general principles discussed in the notes from Subheading 3.2 below can still be used to guide image acquisition.

This chapter outlines detailed steps required for immunolabeling four-color Brainbow samples generated from injection of Cre-dependent Brainbow adeno-associated viruses (AAV) [4] into a transgenic Cre mouse. Following this, a detailed protocol is presented for multispectral imaging of these samples with a laser scanning confocal microscope. Lastly, steps to perform linear unmixing of two of the specific fluorophores in this example are presented. While other microscope systems can be used for image acquisition (such as epifluorescent, spinning disk confocal, multiphoton excitation, or light sheet microscopes), the laser scanning confocal microscope provides optimal resolution in all three dimensions, more flexible in fine-tuning imaging parameters, and are generally more accessible to researchers than light sheet microscopes. In general, Brainbow AAV can produce more hues in a sample than a transgenic animal with a few tandem cassettes inserted into the same genomic locus. This is due to [1] many AAV particles that can infect in the same cell, and [2] while inter-cassette excision can happen in the animal with strong and prolonged Cre activity to reduce the total Brainbow cassette number, the Brainbow cassettes in different AAV particles are exempt from such excision. Moreover, as the Brainbow AAV can also be co-injected with a Cre-expressing AAV, this strategy can be used in any model organism that is subjected to AAV infection. Therefore, this approach is the most robust and accessible way to achieve the highest-quality three-dimensional image data sets from Brainbow samples.

2 Materials

Prepare all solutions in deionized water. Be sure to follow proper chemical waste disposal guidelines, especially regarding paraformaldehyde and sodium azide.

Table 1
Currently available Brainbow tools

Tool (ref)	Genome integration	Recombinase	Promoter	Default	Outcomes	Antibody compatible
<i>Mouse</i>						
Brainbow 1.0 [1]	Transgenic	Cre	Thy1	RFP	YFP, CFP _{mem}	N
Brainbow 1.1 [1]	Transgenic	Cre	Thy1	OFF	RFP _{mem} , YFP _{mem} , CFP _{mem}	N
Brainbow 2.1 [1]	Transgenic	Cre	Thy1	GFP _{nuc}	RFP, CFP _{mem} , GFP _{nuc} , YFP	N
Brainbow 3.0 [4]	Transgenic	Cre	Thy1	mOrange2 _{mem}	EGFP _{mem} , mK2 _{mem}	Y
Brainbow 3.2 [4]	Transgenic	Cre	Thy1	NFP _{nuc}	mOrange2 _{mem} , EGFP _{mem} , mKate2 _{mem}	Y
FLPbow 1 [4]	Transgenic	FLP	Thy1	tdTomato	PhiYFP, ECFP	Y
FLPbow 2 [4]	Transgenic	FLP	Thy1	NFP _{nuc}	mOrange2 _{mem} , EGFP _{mem} , mK2 _{mem}	Y
Autobow [4]	Transgenic	Cre	Thy1	Cre ^a	mCerulean, PhiYFP, mK2	Y
Confetti [8]	Rosa26 knock-in	Cre	CAG	GFP _{nuc}	YFP, CFP _{mem} , RFP	N
R26-Rainbow [20]	Rosa26 knock-in	Cre	CAG	mCherry	mOrange, mCerulean, EGFP	N
Rainbow [21]	Rosa26 knock-in	Cre	CMV/B-act	tdTomato	mCerulean, YFP	N
Ubow [22]	Transgenic	Cre	UbiC	tdTomato	YFP, CFP	N
<i>Drosophila</i>						
Flybow 1.1 [6]	Transgenic	FLP	Gal4/UAS	EGFP _{mem}	EGFP _{mem} , mCitrine _{mem} , Cerulean _{mem} , mCherry _{mem}	N
Flybow 2.0 [6]	Transgenic	FLP	Gal4/UAS	lamin-2xHA	EGFP _{mem} , mCitrine _{mem} , Cerulean _{mem} , mCherry _{mem}	N
dBrainbow [11]	Transgenic	Cre	Gal4/UAS	None	EGFP, EBFP, mKO2	N

LOLLibow [23]	Transgenic	Cre ^b	Gal4/UAS	OPF	mCherry, EYFP, mCerulean	N
TIE-DYE [24]	Transgenic	FLP	Act5C + Gal4/UAS	None	GFP _{nuc} , LacZ _{nuc} , RFP	Y
MCFO [25]	Transgenic	FLP	Gal4/UAS	None	smGFP _{myc} , HA, V5, FLAG, OLLAS ^c	Y
Raepli [7]	Transgenic	PhiC31	Gal4/UAS and/or LexA/LexO	None	TagBFP, mTFP1, mOrange, mKate2 ^d	Y
<i>Zebrafish</i>						
Brainbow (gal4) [26]	Transgenic	Cre	Gal4/UAS	tdTomato	Cerulean, YFP	N
ubi:Zebrabow [27]	Transgenic	Cre	ubi	tdTomato	Cerulean, YFP	N
PriZm [28]	Transgenic	Cre	B-act	tdTomato	Cerulean, YFP	N
<i>Viral vectors</i>						
Brainbow AAV [4]	NA	Cre	EF1 α	None	EYFP _{mem} , TagBFP _{mem} , mTFP1 _{mem} , mCherry _{mem}	Y
HSV-Brainbow [9]	NA	Cre	VGLUT1	EmGFP	mOrange2, LSSmKate2, EBFP2	N
RGB LeGO (lentivirus) [29]	Transduction	None	SFFV	None	mCherry, Venus, mCerulean	N
Rainbow PRV [10]	NA	None	CMV	None	ECFP, mTFP1, EGFP, EYFP, mCherry ^d	Y ^e
<i>rDNA vectors</i>						
Cytbow ^f [5]	Transposase insertion	Cre	CAG	EBFP2 _{nuc}	tdTomato, mCerulean/mTq2, EYFP	N
Nucbow ^f [5]	Transposase insertion	Cre	CAG	EBFP2 _{nuc}	tdTomato _{nuc} , mCerulean _{nuc} , EYFP _{nuc}	N
Palmbow ^f [5]	Transposase insertion	Cre	CAG	EBFP2 _{nuc}	tdTomato _{mem} , mCerulean _{mem} , EYFP _{mem}	N
Mitbow ^f [5]	Transposase insertion	Cre	CAG	EBFP2 _{nuc}	tdTomato _{mito} , mCerulean _{mito} , EYFP _{mito}	N

(continued)

Table 1
(continued)

Tool (ref)	Genome integration	Recombinase	Promoter	Default	Outcomes	Antibody compatible
CLoNe [30]	Transposase insertion	Cre	CAG	None	mSapphire, EGFP, EYFP, mCherry	N
Multibow [31]	Transposase insertion	Cre	actb2	None	EBFP2, Cerulean, EGFP, mCitrine, mKO, tdTomato, mKate2	Y ^c
<i>Arabidopsis</i>						
Bro. of Rainbow [12]	Transgenic	Cre	35S	vYFP _{nuc}	CyPet _{ER} , TagRFP _{ER}	N

The table is organized by species. For those using transposase insertion into the genome, electroporation is used as the method of plasmid delivery. The default state of each design is what is expressed in the absence of the recombinase, some of which are nonfluorescent but can act as an antigen for immunohistology

Nuc nuclear targeted, *mem* membrane targeted, *ER* endoplasmic reticulum targeted, *mito* mitochondria targeted, *PRV* pseudorabies virus, *HSV* herpes simplex virus, *AAV* adeno-

associated virus, *rDNA* recombinant DNA plasmid

^aCre is expressed transiently until recombination, at which point it is self-excised

^bUsed in combination with light-inducible split Cre

^cSpaghetti monster GFPs (smGFPs) act as epitope scaffolds for immunolabeling. MCFO uses epitope combinations selected from five smGFPs. Each with a different epitope tags

^dMultiple cellular domains available for all FPs

^eWith proper combination of FP units (see Table 2)

^fThese constructs, used separately or together, comprise the MAGIC system

2.1 Immunohistology

1. 0.1 M phosphate-buffered saline, pH 7.4 (PBS).
2. 4% paraformaldehyde (PFA): In a chemical fume hood, add 16% w/v PFA to water. Gently stir while heating until temperature reaches 55–60 °C. Slowly add 1 M NaOH to raise the pH until the PFA completely enters the solution (should turn clear). Slowly readjust the pH back to 7.4 with 1 M HCl. This stock solution can be stored at –20 °C for several months. Just prior to use, thaw 16% stock at 50 °C until clear, and then dilute to 4% in PBS. This can be stored at 4 °C for 1–2 weeks, at which point it begins to degrade.
3. Vibratome (Leica VT1000S or other compatible models).
4. 12-well plate (or similar staining vessel).
5. Orbital shaker.
6. StartingBlock, PBS variant (Thermo Fisher).
7. Triton X-100.
8. Heparin.
9. Sodium azide.
10. Primary antibodies: chicken anti-EGFP, rabbit anti-mCherry, rat anti-mTFP1, and guinea pig anti-TagRFP (*see Note 1*). Dilute all primary antibodies together in one cocktail at 1:500 in PBS with 0.5% Triton X-100, 0.2% sodium azide, and 10 µg/mL heparin (*see Note 2*).
11. Parafilm “M” wax film.
12. Highly cross adsorbed (*see Note 3*) secondary antibodies (*see Note 4*): donkey anti-chicken IgY Alexa488 (Jackson ImmunoResearch), donkey anti-guinea pig IgG CF555 (Sigma Aldrich), donkey anti-rat IgG Alex594 (Jackson ImmunoResearch), and donkey anti-guinea pig IgG CF647 (Sigma Aldrich). Dilute all secondary antibodies together in one cocktail each to a final concentration of 2 µg/mL in PBS with 0.5% Triton X-100, 0.2% sodium azide, and 10 µg/mL Heparin (*see Note 2*).
13. Vectashield anti-fade mounting medium (Vector Labs).
14. Glass microscope slides.
15. #1.5 (170 µm) coverslips.
16. Nail polish or coverslips sealant.

2.2 Image Acquisition

1. 488/543/633 dichroic.
2. Laser scanning confocal microscope with 488, 543, and 633 laser lines.

2.3 Linear Unmixing

1. Fiji (NIH).

3 Methods

3.1 Immunohistology

1. Following your institute's guidelines for animal care, perfuse the mouse under heavy anesthesia with cold PBS followed by cold 4% PFA. Dissect the brain and postfix in 4% PFA with gentle shaking at 4 °C overnight. Wash brain with PBS for 1 h with gentle shaking at room temperature (*see Note 5*).
2. Using a Vibratome, cut brain sections up to 100 µm in thickness (*see Note 6*) in the preferred orientation. Collect sections serially in wells of a 12-well plate, returning to the first well after adding sections to every well.
3. Incubate sections in StartingBlock (PBS) with 1.0% Triton X-100 for 4 h at room temperature with gentle shaking (*see Note 7*). This serves as both the blocking and permeabilization step. 12-well plates can be used as the staining vessel, though it is recommended to keep at most two sections (with 600 µL of solution) to three sections (with 750 µL of solution) in each well.
4. Wash in PBS with 0.5% Triton X-100 at room temperature with gentle shaking three times for 30 min each.
5. Add primary antibody cocktail to sections, wrap plate with parafilm, and incubate at 4 °C with gentle shaking for 3–7 days (*see Note 8*).
6. Wash in PBS with 0.5% Triton X-100 at room temperature with gentle shaking three times for 1–2 h each.
7. Add secondary antibody cocktail to sections, wrap plate with parafilm, and incubate at 4 °C with gentle shaking for 1–5 days (*see Note 9*).
8. Wash in PBS with 0.2% Triton X-100 at room temperature with gentle shaking twice for 2 h each.
9. Perform a final wash in PBS at room temperature with gentle shaking for 2 h.
10. Place tissue section on a microscope slide, gently remove excess PBS, and mount sections in excess Vectashield mounting medium (*see Note 10*) between microscope slide and #1.5 coverslips. Place a 2.0 mL microcentrifuge tube filled with water, inverted, on top of the coverslip. Store sample protected from light at room temperature overnight (*see Note 11*).
11. Use vacuum suction or a Kimwipe tissue to remove excess Vectashield from around the coverslip. Seal the sample with clear nail polish. Tissue can be imaged immediately or stored at 4 °C protected from light for at least 1 year.

3.2 Image Acquisition

The methods described here are optimized for secondary antibodies conjugated with Alexa488, CF555, Alexa594, and CF647 (*see* Fig. 2). If using Brainbow samples containing only three FPs, it is best to omit the Alexa594 to eliminate the need for linear unmixing of the 594 and 647 emission signals (*see* Subheading 3.3).

1. Choose the microscope objective (*see* Note 12).
2. Set pixel dimension in (x, y) (*see* Notes 12 and 13).
3. Set the Z -step interval (*see* Note 14).
4. Place the 488/543/633 dichroic in the beam path.
5. Set the minimum and maximum Z coordinates.
6. Set emission collection ranges for each channel (*see* Fig. 2). Collect Alexa488 emission between ~ 500 and 530 nm (Channel 1),

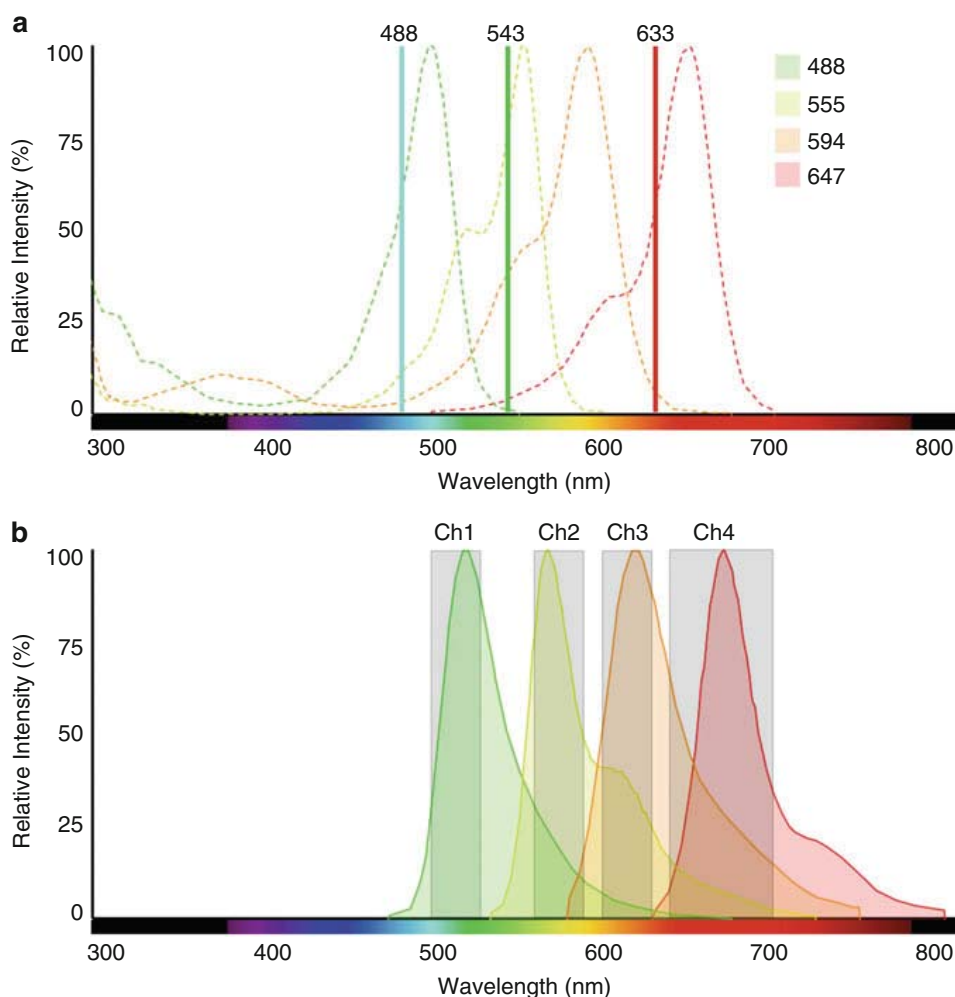


Fig. 2 Imaging spectra. (a) Excitation spectra (*dashed lines*) and excitation wavelengths (*vertical solid lines*) for chosen dyes. (b) Emission spectra and collection ranges (*gray boxes*). For clarity, these emission spectra represent the maximum emission efficiency and are not normalized to the particular laser lines used for the acquisitions described here. These spectra were generated using Thermo Fisher's Fluorescence Spectra-Viewer using the Alexa version of these four dyes (their CF counterparts have similar spectra)

CF555 between ~560 and 590 nm (Channel 2), Alexa594 between ~600 and 630 nm (Channel 3), and CF647 between ~640 and the upper limit of detector (Channel 4).

7. Separate lasers and emission channels into two separate acquisition tracks, 488 and 633 laser lines with Channels 1, 3, and 4 onto Track 1, and assign the 543 laser and Channel 2 onto Track 2 (*see Note 15*).
8. Set pinhole diameter to match the diameter of the expected Airy disk for optimal signal-to-noise ratio (*see Note 16*). Some acquisition software, such as Zeiss' Zen, can set this automatically, or it can be calculated with the following equation [14]:

$$d_{\text{Airy}} = \frac{1.22 \times \lambda}{\text{N.A.}} \times M \times C$$

where λ = mean wavelength of the three excitation lasers, N.A. is the numerical aperture of the objective, M is the magnification of the objective, and C is the magnification of optical components in the confocal head (different for each confocal system but can be obtained from the manufacturer).

9. Set the gain on the detector (*see Note 17*).
10. Set the laser power for each laser (*see Note 17*). Because a large proportion of emitted photons from the Alexa594 fluorophore will be collected in Channel 4, adjust the laser power for both fluorophores according to the Channel 4 intensity alone (Channel 3 can appear comparatively dim until unmixing). If the acquisition software has a function for correcting intensity in depth, set the optimal laser power at the top and bottom of the Z-stack. This will compensate for the loss of excitation due to light absorption and scattering through the tissue.
11. Set the refractive index correction ratio by dividing the refractive index of the mounting medium (1.45 for Vectashield in this case) by the refractive index of the submersion media (oil, water, air, etc.).
12. Set the pixel dwell time and use averaging across two scans (*see Note 17*). For this step it is best to take a few scans using different dwell time/averaging settings to determine the minimum scan time required for the desired image quality.
13. Run the acquisition, checking occasionally to be sure the system has not failed.

3.3 Linear Unmixing

For the fluorophores and parameters described here, some unmixing must be done post-acquisition to effectively remove the Alexa594 emission from Channel 4 and add it back to Channel 3 (*see Fig. 3*). In confocal microscopes equipped with array spectral

detectors, such as the Zeiss LSM780 or LSM880, this can be done using lambda scan mode combined with “online fingerprinting” function. The image processing steps below will be required for other microscope systems. These instructions are intended for the Fiji version of ImageJ [15]:

1. Directly apply ~5–10 μL of a 1:500 dilution of Alexa594 secondary antibody directly to a coverslip and mount to a slide.
2. Acquire a reference image from this slide using the *exact* same imaging settings as in Subheading 3.2 for Channels 3 and 4 except for the laser intensity, which can be adjusted (*see Note 18*). Again, the ideal image will have the maximum pixel values ~80% of the maximum dynamic range (*see Note 17*). For this the Channel 1 and 2 should be omitted as should the 488 and

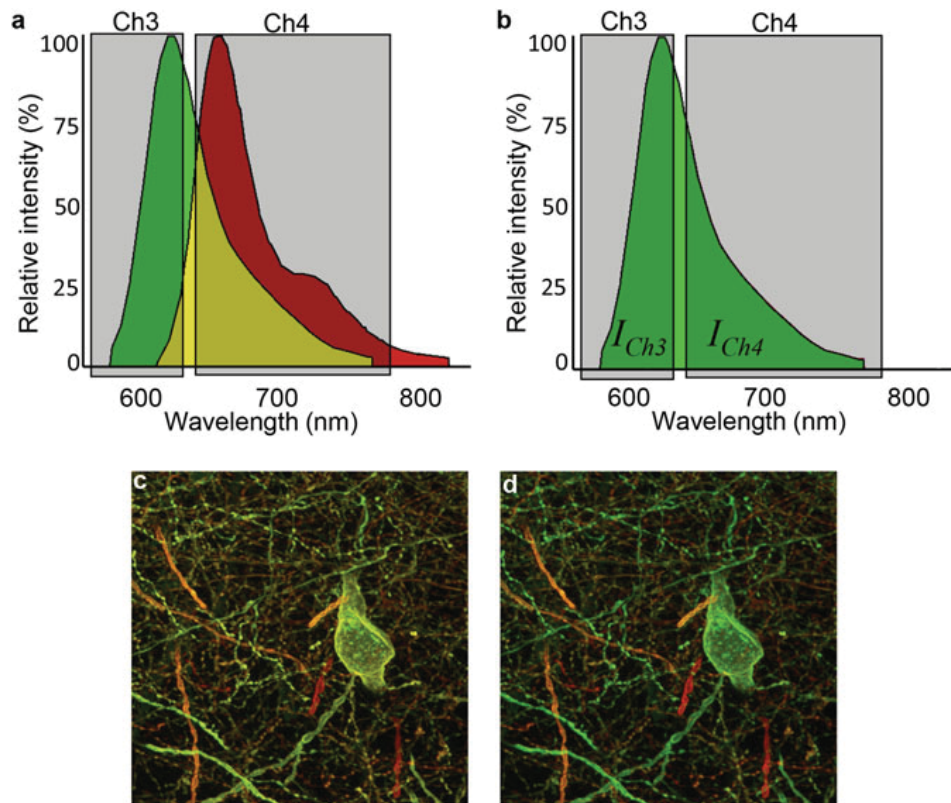


Fig. 3 Unmixing of Alexa594 and CF647 emission. (a) Photon emission from Alexa594 (*green*) overlaps with emission from CF647 (*red*) shown here in the yellow region. Gray boxes representing the emission collected in Channels 3 and 4 demonstrate the large portion of Alexa594 emission collected in Channel 4 which can be recovered through linear unmixing. (b) A reference spectrum is obtained by capturing an image of the Alexa594 dye using identical imaging conditions. The area under the Alexa594 emission curve in each channel (I_{Ch3} and I_{Ch4}) is used to calculate the ratio of Alexa594 to CF647 emission collected in Channel 4 (*yellow region* under the gray Ch4 box in a) and to correct the values in the raw data. (c) The maximum Z-projection of an image stack prior to unmixing shows significant overlap between Channel 3 (*green*) and Channel 4 (*red*). (d) After unmixing the color separation is restored as evidenced by the large number of structures that become a “*pure green*” color

543 lasers. Remove the slide and acquire a second image with the same setting as background noise, this time using the same laser power as the reference image as well.

3. Open each image in Fiji and run the “Process > Subtract Background” function for each, and then calculate the mean pixel intensity across each of these two reference images. This can be done using the “Analyze > Measure” tool. These values will serve as I_{BG} , I_{Ch3} , and I_{Ch4} in **steps 4–6**.
4. Calculate the value α to use in **steps 5–6**:

$$\alpha = \frac{I_{Ch4}}{I_{Ch3}}$$

5. Open Channel 3 from the Brainbow Acquisition in Subheading 3.2 as a Separate Image Stack. Apply the Following Calculation:

$$Img_{594} = (Img_{Ch3} - I_{BG}) \times (1 + \alpha)$$

where Img_{Ch3} is the raw image stack and Img_{594} is the resulting unmixed 594 emission image stack. This can be accomplished in Fiji by first choosing “Process > Math > Subtract” and entering I_{BG} . Next, use “Process > Math > Multiply” and enter the $1 + \alpha$ value. Save this as a separate new image stack (Img_{594}) as the original raw Channel 3 image stack will be needed again in the next step.

6. Open the Original raw Channel 3 and Channel 4 Data as Separate Image Stacks. Perform the Following Calculation:

$$Img_{647} = (Img_{Ch4} - I_{BG}) - (Img_{Ch3} \times \alpha)$$

subtract I_{BG} from Img_{Ch4} as in **step 5**. Then, being sure to select Img_{Ch3} as the active window, use the “Process > Math > Multiply” function entering the value for α . Perform the final subtraction using “Process > Image Calculator (choose ‘Subtract’),” and select the proper image stacks for the operation. Save this as a new image stack (Img_{647}).

7. Open Channel 1, Channel 2, Img_{594} , and Img_{647} as separate image channels, and use the “Image > Color > Merge Channels” to make a new composite image stack.
8. If signal intensity varies greatly along the Z axis, perform histogram matching to produce homogenous color in depth. Add a slice to the very front of the image stack: “Image > Stacks > Add Slice (check ‘Prepend’).” Next, find a slice in which one channel has the best overall contrast. Select that channel and select the whole image frame, copy the content of that channel, and

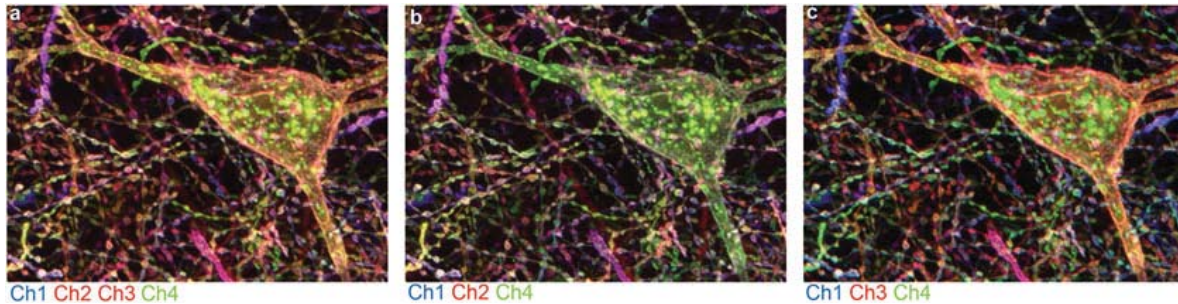


Fig. 4 Displaying four channel images. **(a)** Images can be displayed by either combining two channels into one display color or by toggling displaying one of two channels assigned to the same color (compare **(b)** and **(c)**)

Table 2
Antigenicity of primary FP antibodies

Antibody	Validated antigens
Chicken, anti-EGFP IgY	EBFP2, ECFP, Cerulean, Venus, mCit, EGFP, sfGFP, EYFP, mAmetrine
Rabbit, anti-mCherry serum	DsRed, mOrange2, tdTomato, mCherry
Rat, anti-mTFP1 serum	mTFP1, mWasabi
Guinea pig, anti-TagRFPt serum	TagBFP, TagRFP, TagRFPt, mKate2, tdKatushka2, eqFP650

While other FPs derived from similar species are predicted to serve as antigen for the same primary antibody (e.g., mEmerald and EGFP are both derived from *Aequorea victoria* and thus mEmerald is predicted to serve as antigen for the chicken anti-EGFP primary), only these have been directly validated by the authors

paste it to the first channel in the first slice. Now run “Image > Adjust > Bleach Correction (‘Match Histogram’),” followed by “Plugins > Image Normalizer (‘Stack Maximum’).” Save as a new image stack.

- The final composite image stack can be viewed in a variety of different color display configurations (*see* Fig. 4) (*see* **Note 19**), but regardless adjustments to the brightness and contrast independently of each channel will likely be needed to give the best color balance to the human eye.

4 Notes

- While these were the purified FPs used to generate the primary antibodies, the primaries also bind to FP variants derived from the same organism species. See Table 2 for a complete list of FP antigens for each of these primary antibodies. These four primary antibodies are custom produced in the Cai Lab and are distributed through Kerafast. Though similar primary antibodies may be commercially available elsewhere, they need to be validated with this protocol.

2. The Heparin is optional, though it can decrease nonspecific/background binding of antibodies in the tissue, most notable in the blood vessels. This is especially important in sparsely labeled samples where primary antibody can be in excess of antigen.
3. Secondary antibodies should be cross adsorbed by the manufacturer to eliminate nonspecific binding to IgG from other primary species.
4. The choice of secondary antibodies may vary depending on the optics of the available microscope. The cocktail of secondary antibodies in this protocol was chosen to optimize the speed of image acquisition while limiting the amount of spectral cross talk between fluorophores (see Subheading 3.2). While Alexa dyes can also be used in place of the two CF dyes here, there are two notes of caution: first, the CF647 is brighter than the Alexa647, and second, while the Alexa546 has stronger excitation with 543 nm laser light, it tends to aggregate on the surface of the tissue.
5. Brains can be stored in PBS with 0.2% sodium azide for at least several months before or after sectioning. While fluorescence intensity may decrease during long-term storage, the antigenicity of the FPs still remains, and thus the tissue is still suitable for immunohistology.
6. Floating sections are required for this histology protocol for optimal antibody penetration through both sides of the tissue. This protocol can reliably achieve complete antibody penetration through a 100 μm brain section from mice up to ~4 months of age. Over the lifetime of the mouse, lipid accumulation in the brain hinders complete penetration, and thus 60–80 μm sections are recommended for older mice. While the prevalence of whole organ and/or thick tissue immunohistology and clearing techniques is rapidly increasing, they are still improving and emerging and are therefore omitted from this protocol for simplicity. If imaging of thicker sections is desired, other methods, such as 3DISCO [16] and iDISCO (non-methanol variation) [17], can be used in place of this protocol for immunohistology. One caution to note is that when using clearing techniques such as CLARITY [18], which use harsh detergent conditions to strip lipids from the tissue after cross-linking proteins to a gel-like matrix, much of the plasma membrane-bound protein (such as those used in many Brainbow reagents) are often removed as well. Therefore, it is recommended to immunolabel tissue prior to clearing.
7. The StartingBlock product produces superior results compared to other blocking reagents (i.e., various serums) as this proprietary formula purportedly blocks against nonspecific binding from antibodies raised in most commonly used species.

8. The incubation time depends on the thickness of the section and the age of the mouse from which it was collected (in other words, the amount of lipid in the brain), both of which can hinder complete and homogenous antibody penetration through the sample. For 100 μm sections from adult mice 2–4 months of age, incubate for 7 days; for thinner sections from adult mice, incubate for 5 days; for sections from neonates, the incubation time can be shortened to 3 days regardless of thickness. Incubation times can be ~halved if incubations are done at room temperature with gentle shaking, though tissue degradation can occur if tissue fixation is suboptimal. If immunolabeling still appears incomplete in the middle of the section, it is also possible that the antibodies are becoming depleted before they reach the center of the tissue. It is therefore recommended to replenish and/or supplement with fresh antibodies half way through the incubations or to increase the volume of antibodies added to the tissue.
9. The incubation times for secondary antibodies can be shorter than for the primaries because the binding affinities are much higher. Determining the time for the specific sample follows the same general guidelines as in **Note 5** for primary antibodies, but standard practice is ~half the time used for primary antibody incubation.
10. Vectashield is an anti-fading reagent supplement, aqueous-based, nonsolid-forming mounting media with a refractive index of 1.45. While mouse brain has a refractive index of ~1.48–1.49, laser light generally passes through sections up to 100 μm with a manageable amount of scattering. It is also available with DAPI if desired. Alternatively, RapiClear (SunJin Labs), a nonsolid-forming mounting media with a refractive index of 1.47, can be used to further increase the clearness of sections [19] up to 300 μm thick.
11. Placing a weight on top of the section prevents it from curling during the exchange of water/PBS in the tissue and glycerol in the Vectashield.
12. One basic parameter to consider before setting up a confocal image acquisition is the desired resolution/pixel size. This will largely depend on the specific biological question, but in general increasing resolution will come at a cost in acquisition time and data size. While in some cases, these trade-offs may indeed be trivial, in circumstances where imaging a large volume of tissue is desired, acquisition times can extend over periods of days, while data size can easily reach the hundreds of gigabyte scale. In addition, increasing scan time per frame increases the risk of photobleaching the sample.

13. While the minimum (x, y) pixel size in diffraction-limited microscopy is ~ 200 nm, oversampling to about 100–150 nm is optimal if deconvolution is to be used in post-acquisition processing.
14. The axial resolution in the confocal system depends on the numerical aperture of the objective and the size of the pinhole. In practice, it is generally assumed that the maximum resolution in the Z dimension is approximately twice the X and Y resolution. Therefore the minimum Z -step size should be about twice the size of the (x, y) pixel size. If performing downstream deconvolution, oversampling is recommended in Z as well.
15. Acquisition tracks allow for excitations and emissions to be collected independently from one another. This prevents fluorophore cross talk as CF555 can be excited by 488 nm laser light and CF555 emission will bleed into the Alexa594 emission range. Tracks use either a “line switching” mechanism, in which the lasers and channels are alternated after each line scan in X across the frame, or a “frame switching” mechanism where each entire frame is collected before switching tracks. If unable to use a single dichroic for excitation as described here, frame switching is required and can more than double acquisition time owing to the need to physically change the dichroic mirror between each track.
16. Dim samples may benefit from an increased pinhole beyond the Airy disk diameter at the expense of decreased resolution. This is especially true for sparsely labeled samples where interference from out-of-focus light is less of a concern.
17. There are a variety of illumination/detection parameters that contribute to the overall signal-to-noise ratio. Which settings are optimal will depend on how bright the sample is and how much noise can be tolerated for each particular experiment. The main contributing factors are the gain on the detector, the laser power, and the pixel dwell time (i.e., speed of scanning). Setting a high gain on the detector will increase image signal but at the cost of increasing noise. This can be offset by using longer pixel dwell times and/or averaging multiple scans, but this comes at the cost of acquisition time. Increasing laser intensity is the simplest way to maximize the signal-to-noise ratio, yet photobleaching can become an issue in thicker samples. While it is often in the user’s best interest to obtain the strongest signal from the sample, it is important to set parameters properly so that the maximum pixel intensity in the image is equal or smaller than 80% of the total dynamic range to assure the strong signals fall into the detector’s linear detection range. For example, the dynamic range of a 12-bit image

contains a maximum intensity value of 4000, so the highest pixel value in the image should be ~3200. This is particularly important if unmixing is to be performed as saturation of detector will cause unmixing errors.

18. What will be calculated for unmixing Channel 3 and 4 is the ratio between the areas under the 594 and 647 emission curves collected in Channel 4 (*see* Fig. 3). In order to keep the unmixing parameter as a constant, all imaging parameters, with the exception of laser power, must be unchanged between taking the reference images and sample images. While changing laser power will proportionally change the intensity in Channel 3 and 4 (i.e., constant ratio), changing other parameters will have nonlinear effects to the average intensity in each image.
19. As a computer monitor can only compose pixel outputs based on red, blue, and green channel information, special consideration needs to be made for displaying data from four channels/colors. There are two ways to approach this: one is to combine two channels to the same color and display all four simultaneously. However, this limits the true power of four-color Brainbow labeling. An alternative approach is to assign two channels to the same color and toggle between displaying only one of them when trying to resolve color ambiguities between structures from different cells (*see* Fig. 4).

References

1. Livet J et al (2007) Transgenic strategies for combinatorial expression of fluorescent proteins in the nervous system. *Nature* 450 (7166):56–62
2. Branda CS, Dymecki SM (2004) Talking about a revolution: the impact of site-specific recombinases on genetic analyses in mice. *Dev Cell* 6 (1):7–28
3. Lichtman JW, Livet J, Sanes JR (2008) A technical approach to the connectome. *Nat Rev Neurosci* 9(6):417–422
4. Cai D, Cohen KB, Luo T, Lichtman JW, Sanes JR (2013) Improved tools for the Brainbow toolbox. *Nat Methods* 10(6):540–547
5. Loulier K et al (2014) Multiplex cell and lineage tracking with combinatorial labels. *Neuron* 81(3):505–520
6. Hadjiconomou D et al (2011) Flybow: genetic multicolor cell labeling for neural circuit analysis in *Drosophila melanogaster*. *Nat Methods* 8(3):260–266
7. Kanca O, Caussinus E, Denes AS, Percival-Smith A, Affolter M (2014) Raeppli: a whole-tissue labeling tool for live imaging of *Drosophila* development. *Development* 141 (2):472–480
8. Snippet HJ et al (2010) Intestinal crypt homeostasis results from neutral competition between symmetrically dividing Lgr5 stem cells. *Cell* 143(1):134–144
9. Zhang G-R et al (2015) Neurons can be labeled with unique hues by helper virus-free HSV-1 vectors expressing Brainbow. *J Neurosci Methods* 240:77–88
10. Boldogkoi Z et al (2009) Genetically timed, activity-sensor and rainbow transsynaptic viral tools. *Nat Methods* 6(2):127–130
11. Hampel S et al (2011) *Drosophila* Brainbow: a recombinase-based fluorescence labeling technique to subdivide neural expression patterns. *Nat Methods* 8(3):253–259

12. Wachsman G, Heidstra R, Scheres B (2011) Distinct cell-autonomous functions of RETINOBLASTOMA-RELATED in Arabidopsis stem cells revealed by the brother of Brainbow clonal analysis system. *Plant Cell* 23(7):2581–2591
13. Weissman TA, Pan YA (2015) Brainbow: new resources and emerging biological applications for multicolor genetic labeling and analysis. *Genetics* 199(2):293–306
14. Conchello J-A, Lichtman JW (2005) Optical sectioning microscopy. *Nat Methods* 2(12):920–931
15. Schindelin J et al (2012) Fiji: an open-source platform for biological-image analysis. *Nat Methods* 9(7):676–682
16. Ertürk A et al (2012) Three-dimensional imaging of solvent-cleared organs using 3DISCO. *Nat Protoc* 7(11):1983–1995
17. Renier N et al (2014) iDISCO: a simple, rapid method to immunolabel large tissue samples for volume imaging—suppl original. *Cell* 159:896–910. <http://www.sciencedirect.com/science/article/pii/S0092867414012975>.
18. Chung K, Deisseroth K (2013) CLARITY for mapping the nervous system. *Nat Methods* 10(6):508–513
19. Seiradake E et al (2014) FLRT structure: balancing repulsion and cell adhesion in cortical and vascular development. *Neuron* 84(2):370–385
20. Rinkevich Y, Lindau P, Ueno H, Longaker MT, Weissman IL (2011) Germ-layer and lineage-restricted stem/progenitors regenerate the mouse digit tip. *Nature* 476(7361):409–413
21. Tabansky I et al (2013) Developmental bias in cleavage-stage mouse blastomeres. *Curr Biol* 23(1):21–31
22. Ghigo C et al (2013) Multicolor fate mapping of Langerhans cell homeostasis. *J Exp Med* 210(9):1657–1664
23. Boulina M, Samarajeewa H, Baker JD, Kim MD, Chiba A (2013) Live imaging of multicolor-labeled cells in *Drosophila*. *Development* 140(7):1605–1613
24. Worley MI, Setiawan L, Hariharan IK (2013) TIE-DYE: a combinatorial marking system to visualize and genetically manipulate clones during development in *Drosophila melanogaster*. *Development* 140(15):3275–3284
25. Nern A, Pfeiffer BD, Rubin GM (2015) Optimized tools for multicolor stochastic labeling reveal diverse stereotyped cell arrangements in the fly visual system. *Proc Natl Acad Sci U S A* 112(22):E2967–E2976
26. Robles E, Filosa A, Baier H (2013) Precise lamination of retinal axons generates multiple parallel input pathways in the tectum. *J Neurosci* 33(11):5027–5039
27. Pan YA et al (2013) ZebraBow: multispectral cell labeling for cell tracing and lineage analysis in zebrafish. *Development* 140(13):2835–2846
28. Gupta V, Poss KD (2012) Clonally dominant cardiomyocytes direct heart morphogenesis. *Nature* 484(7395):479–484
29. Weber K et al (2011) RGB marking facilitates multicolor clonal cell tracking. *Nat Med* 17(4):504–509
30. García-Moreno F, Vasistha NA, Begbie J, Molnár Z (2014) CLoNe is a new method to target single progenitors and study their progeny in mouse and chick. *Development* 141(7):1589–1598
31. Xiong F, Obholzer ND, Noche RR, Megason SG (2015) Multibow: digital spectral barcodes for cell tracing. *PLoS One* 10(5):e0127822